ACERP: Vol. 6, No. 3, (Summer 2020) 47-54

Advanced Ceramics Progress

Research Article

Journal Homepage: www.acerp.ir

Synthesis of a Macroporous Glass-Ceramic Scaffold Containing Fluorapatite Crystalline Phase for Bone Substitutes

M. Rezvani [a *], E. Alahgholiyan [a], L. Roshangar [b]

[a] *Department of Materials Engineering, Faculty of Mechanical Engineering, University of Tabriz, Tabriz, Iran*
[b] *Histology and Embryology Stem Cell Research Center, Tabriz University of Medical Sciences, Tabriz, Iran*

PAPER INFO

Paper History:

Received 02 June 2019
Received in revised form 16 July 2019
Accepted 16 August 2019

Keywords:

Glass-Ceramic
Fluorapatite
Macroporous
Porogen

ABSTRACT

Bioactive glass-ceramics play an important role in bone tissue regeneration. In the present research, the crystallization of glasses and scaffold fabrication were investigated. After choosing the appropriate composition in the SiO_2-CaO-Na_2O-P_2O_5 system, raw materials were melted at 1400℃ and then, quenched in water. Subsequently, the crystallization of synthesized glass samples was studied. Fourier Transfer infrared (FT-IR) spectroscopy was carried out to study the structural changes of the samples. XRD patterns showed that fluorapatite $Ca_{10}(PO_4)_6(O,F_2)$ was the only precipitated crystalline phase. The template synthesis method was applied for the fabrication of the scaffold and starch as a porogen material. The optimized scaffold structure was chosen with the appropriate size of pores, interconnectivity, and strength behavior through investigating the porosity, SEM images, and mechanical properties. ICP, SEM, and EDX analyses were used to determine the in vitro bioactivity of the samples after immersion for 14 days in SBF.

1. INTRODUCTION

In recent decades, many types of research have been conducted on orthopedic surgery and bone tissue engineering. The scaffold is a key material in this application, which acts as a matrix for the growth of bone cells [1-7]. For being used as bone grafts, the ideal of scaffold for replacing part of the porous bone is as following:

1) Having 50-60% porosity with interconnected porosity and the average pore size higher than 100μm, so that the cells can easily grow inside and carry the food to the bone.
2) Being made of biocompatible and bioactive materials.
3) Having a rough surface to make the soft tissue more adhesive.
4) Having a simple preparation method that can be prepared in different forms for various damaged areas of the body [1-7].

Therefore, the necessity of a bioactive material for cells growth with a porous structure is inevitable. Most of the bioactive materials used in bone tissue engineering applications are bio-ceramics, such as calcium phosphates, hydroxyapatite (HA), composite materials, metals, glass, and glass-ceramics [8-10]. Bioactive materials can bond to bone tissue through forming a bone-like hydroxyapatite layer on their surface in physiological body fluids (in vitro and in vivo) [7-11]. The advantage of bioactive glasses and glass-ceramics among the different kinds of bioactive materials is the high speed of surface reactions that results in rapid bone formation [10-12]. Glasses and glass-ceramics, which are basically composed of SiO_2, CaO, Na_2O, P_2O_5, have been investigated due to their tunable bioactive behavior. The glass entitled 45S5 Bioglass® (with the composition of $45SiO_2$-$24.5Na_2O$-24.5CaO-$6P_2O_5$ (%wt)) is the most common bioactive glass reported by researchers [8, 13-17].

Recently, various glass-ceramics have been used by researchers for bone repair applications. Three major groups of glass-ceramics that have been examined are apatite-wollastonite, mica-apatite, and Ceravital® [8, 9, 13-18]. The crystalline fluorapatite phase is the most valuable phase for antibacterial and bioactive properties among these glass-ceramics [19-21]. Different methods have been proposed to create porosity in glass-ceramics such as foam synthesis, template synthesis, phase separation method, and freeze extrusion fabrication [22].

* Corresponding Author Email: m_rezvani@tabrizu.ac.ir (M. Rezvani)
https://doi.org/10.30501/acp.2020.113603

The research has focused on the preparation and characterization of a macroporous bioactive glass-ceramic scaffold containing fluorapatite crystals. The fluorapatite phase has not been so far formed by any body in a combination that is nearly 45S5.
To this end, the template synthesis method was used to fabricate the porous structure because this method is the easiest way to control the pores size, the interconnectivity of the pores, and the size distribution of the pores [7, 22]. Moreover, starch was used as a porogen material for being easy crushing and economical.
The main factors affecting the final porous structure and its properties, which have been studied are the total solid loading, particle amount and size of starch powders, consolidation and burning out treatment, and sintering condition.

2. EXPERIMENTAL PROCEDURE

2.1. Synthesis of Glass Samples

The high purity commercially available powders were used as raw materials including Leached SiO_2 with high purity (>99), P_2O_5 (Merck 1005401000), Na_2CO_3 (Merck10639), $CaCO_3$ (Merck102069), and CaF_2 (Dau Jung 2508145). According to reaction 1, the required F ions were prepared by replacing some amounts of CaO with CaF_2. Therefore, the required CaO and F ions were produced simultaneously without changing the composition. As a result, the compositions were prepared with the following weight ratio (%wt) $40SiO_2$, 12CaO, $16.71CaF_2$, $21Na_2O$, $15P_2O_5$.

$$(CaF_2 + ½O_2 = CaO + F_2) \quad (1)$$

The glass frits were prepared by melting raw materials at 1450℃ for 1h in an alumina crucible and quenched in cold water. The frits were dried and milled to particles with the size <40μm. The Fourier transform infrared (FT-IR) spectroscopy (Tensor27, braker, Germany) of the glass and glass-ceramic samples, was used to study the structural changes in the range of 400-1500 cm^{-1}. The thermal behavior of glass powders was determined through differential thermal analysis (DTA-Linseis L181) at the heating rate of 10℃.min^{-1} and the crystalline phase precipitated during sintering were determined through x-ray diffraction (XRD) analysis (Siemens, model D-500). The microstructure of glass-ceramic samples was characterized by a scanning electron microscopy (FE-SEM, Mira-3Tescan).

2.2. Scaffold Fabrication

The scaffolds were fabricated through mixing starch particles and glass powders, with a thermally removable organic material as the pore former. The glass powders, which were sieved below $40\mu m$ and the starch (higher than 99% purity) were carefully mixed for 20min in a plastic bottle using a rolling shaker to obtain an effective mixing. The obtained mixture was blended with 0.4wt% polyvinyl alcohol solution and then, pressed with uniaxial 500MPa pressure to form a pellet with 18mm diameter and 3mm thickness. Drying the pressed specimen was carried out with the gradual increase of the temperature to 100℃ to prevent cracking caused by the sudden drying of the sample.
In this research, the amount of starch was varied in the range of 30-70 vol% to get the best balance between satisfactory sintering temperature, high porosity contact, porosity size, interconnectivity, and mechanical strength. Table 1 represents the experimental parameters applied to the production of each sample.

TABLE 1. Experimental parameters for the production of each sample

Sample code	Temperature(℃)	Starch (vol%)
GCF-615-P30	615	30
GCF-615-P40	615	40
GCF-615-P50	615	50
GCF-615-P60	615	60
GCF-615-P70	615	70
GCF-640-P30	640	30
GCF-640-P40	640	40
GCF-640-P50	640	50
GCF-640-P60	640	60
GCF-640-P70	640	70
GCF-665-P30	665	30
GCF-665-P40	665	40
GCF-665-P50	665	50
GCF-665-P60	665	60
GCF-665-P70	665	70

Finally, the total porosity, open porosity, and bulk density of the samples were investigated and the flexural strength was measured by three-point bending test (Zwieck Roell ZHV10, Germany). The scaffold was studied by the Scanning Electron Microscope (SEM) to evaluate the size, morphology, distribution, interconnectivity, and degree of sintering.

2.3. Chemical Degradation and Apatite Forming Ability

The bioactivity of the samples was evaluated using in vitro tests as explained by Kokubo et al. [23]. The biodegradation and apatite forming ability of the glass-ceramics were investigated by immersion of sintered glass-ceramic discs (with a diameter as much as 10mm) in 50ml simulated body fluid (SBF) solution at 37℃. The experiments were conducted at different time durations between 1 to 14 days. Each test was repeated for 3 times to ensure the accuracy of the results. The glass-ceramic sample was got out of the liquids after each test and then, pH and concentrations of Ca^{2+}, P^{5+},

and Si^{4+} ions were measured using inductively coupled plasma-optical emission spectroscopy (ICP-OES)]. The apatite forming ability on glass-ceramic was studied through the XRD and SEM-EDS analysis.

3. RESULTS AND DISCUSSION

3.1. Crystallization of Glass Samples

DTA curves were studied to determine the crystallization temperatures. Figure 1 illustrates the DTA curves of the compositions after melting and quenching. The peaks of Fluorapatite phase ($Ca_{10}(PO_4)_6(O, F_2)$ (ICDD: 01-077-0120) appeared in the XRD patterns after heat-treating the samples at the first DTA peak temperature for 2h. Figure 2 presents the XRD patterns of glass and glass-ceramic samples. The XRD patterns showed that there were no unwanted phases in the glass sample and after heat-treatment of the samples. Moreover, the peaks of the crystalline phases appeared and the crystallization increased by increasing the temperature.

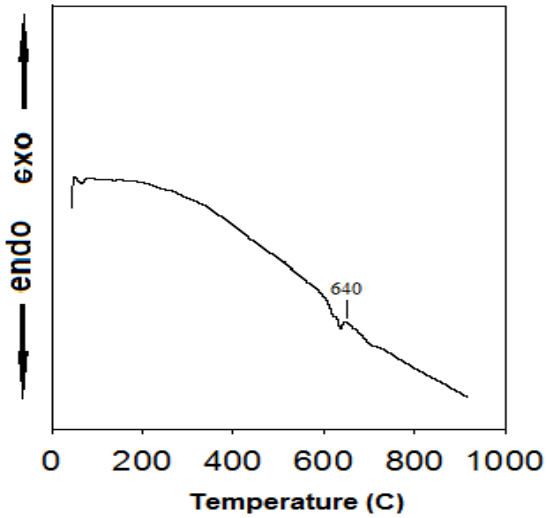

Figure 1. DTA curves of frits with a heating rate of 10℃/min

3.2. Structure of the Glass and Glass-ceramics

The FT-IR spectra of the glass and glass-ceramic samples are illustrated in Figure 3 after heat treatment at 615, 640, and 665°C [24]. The structural information about glass and glass-ceramic can be obtained from these spectra. There were clear peaks that proved the presence of SiO_4 tetrahedrons in the glass network due to the significant amount of SiO_2 in the composition of the samples. The peaks available at ~576.2 and ~765.26cm^{-1} are attributed to the rocking and symmetric stretching vibrations of Si-O-Si bonds, respectively [25].

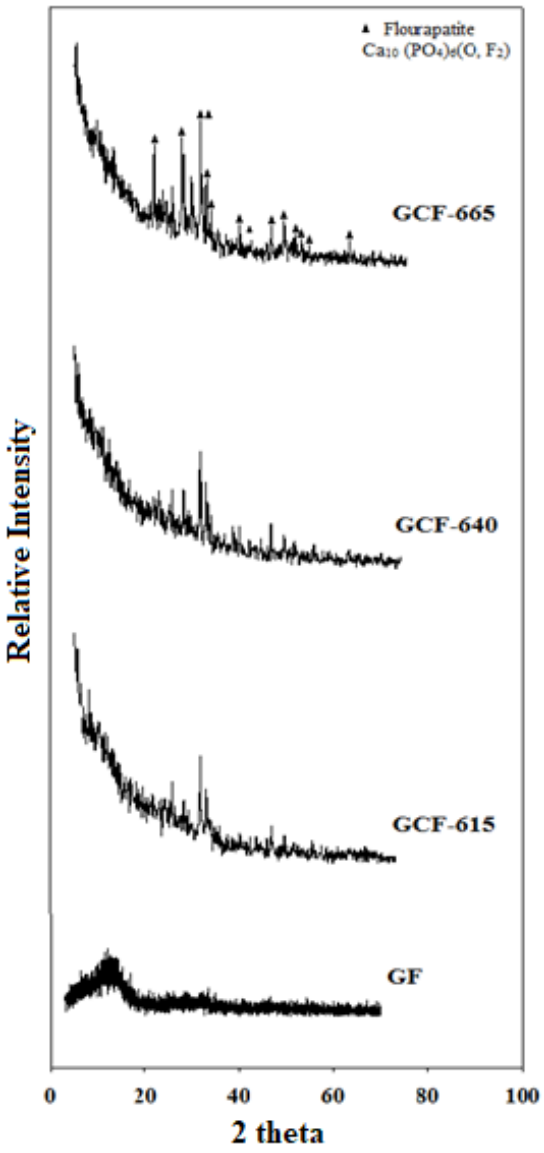

Figure 2. XRD patterns of glass and glass-ceramic heat-treated at different temperatures

As a consequence of overlapping with the rocking vibrations of Si-O-Si, the peaks of Ca-F bond were somehow difficult to be distinguished, although those peaks were reported at ~468.30cm^{-1} [24, 26]. According to [14], it is possible to attribute the peak at ~1025cm^{-1} to this bond. The peak visible in ~1030.27cm^{-1} can also be attributed to the vibrations of Si-O-Ca bond, when the amount of Ca in the glass samples is high (due to the presence of CaF_2 and CaO, simultaneously). As it is reported, there are PO_3 groups due to the network forming the role of P_2O_5 and peaks available in ~577.67 and ~1030cm^{-1} are attributed to PO_3 groups and P-O bonds [27, 28, 29]. It seems that these bonds were available in the samples, but overlapping with Si-O-Si and Si-O-Ca peaks made it difficult to be distinguished.

The intensity of the silicon structure peaks was higher in all investigated glass-ceramics than the base glass. These changes in the peaks can be attributed to a more regular four-dimensional SiO_4 arrangement, symmetric structure, and low-angle variation among the bonds. The intensity of the peaks in crystalline materials was more than amorphous [30].

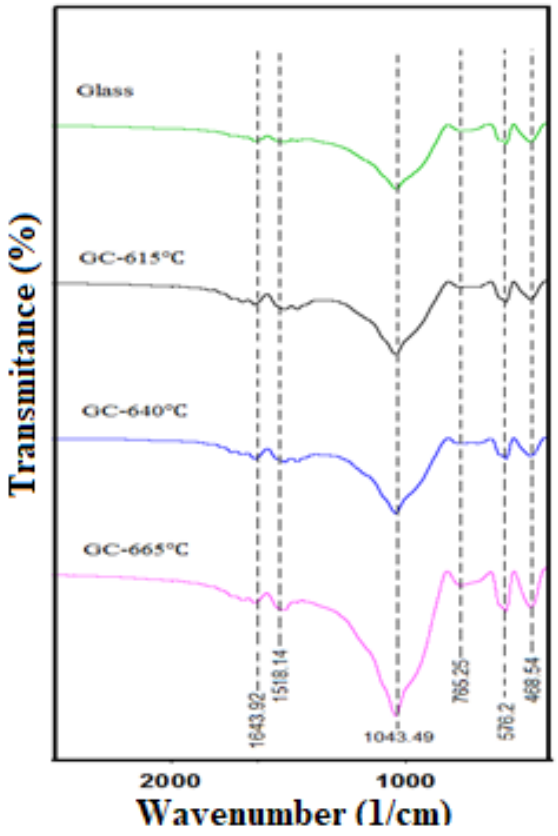

Figure 3. FT-IR spectra of the glass and glass-ceramics heat-treated at 615, 640 and 665℃

3.3. Microstructure Study of Glass-Ceramics

The microstructures of glass-ceramic samples, which were heat-treated at 665℃ for 2h are illustrated in Figure 4. The obvious phase separation can be attributed to crystallization of fluorapatite. It also shows that the morphology of the fluorapatite phase is almost spherical.

Figure 5 shows the results of EDX analysis of bright areas (A in Figure 4) that are fluorapatite crystalline phase (since the peaks of calcium, fluorine, and phosphorus were observed in the EDX pattern).

3.4. Glass-Ceramic Scaffolds (Porosity and Mechanical Properties)

The heat treatment of the samples was performed at 615-665℃ for 2 hours. The total porosity percentages of porous glass-ceramics are shown in Figure 6. The starch was added to glasses from 30 to 70 vol%.

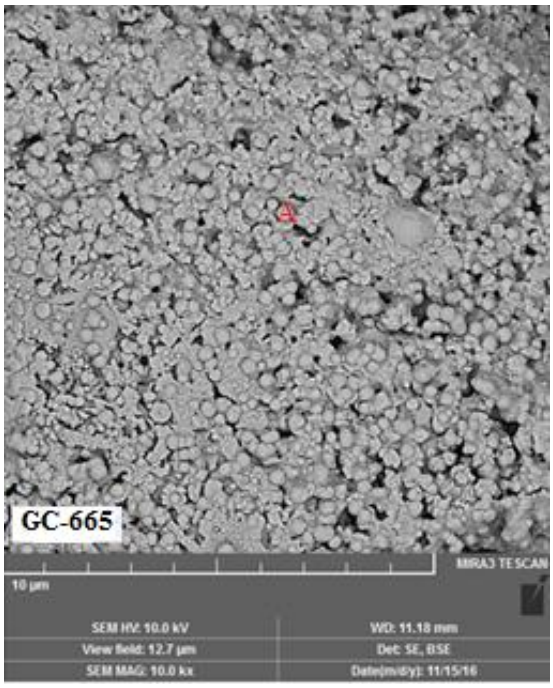

Figure 4. SEM image of glass-ceramic sample heat-treated at 665℃ for 2h

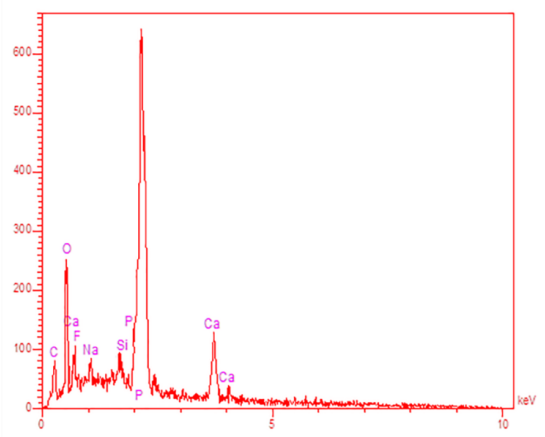

Figure 5. EDX spectrum of fluorapatite crystalline phase

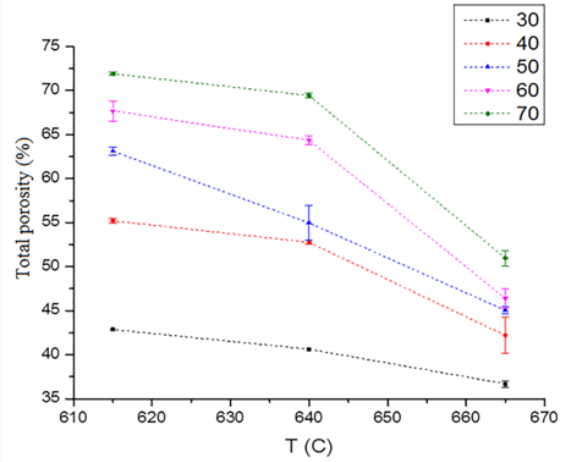

Figure 6. Total porosity percentage of glass-ceramic scaffolds heat-treated for 2h

It is clear that the amount of total porosity and open porosity decrease and the density increases with increasing of temperature and reducing of porogens. According to the results obtained in porous bodies, the GCF-615-P40 (Glass-ceramic fluorapatite, heat-treated at 615℃, starch 40 vol%), GCF-615-P50, GCF-615-P60, GCF-615-P70 samples had not a suitable strength. The flexural strength of the samples GCF-640-P40, GCF-640-P50, and GCF-665-P70 was about 12, 8, and 4MPa, respectively. Considering the previously reported flexural strength, the ranges of the samples are within the acceptable range [31-33].

The samples including GCF-640-P50 (with 58% porosity), GCF-640-P40 (with 55% porosity), and GCF-665-P70 (with 56% porosity) were selected as glass-ceramic scaffolds for bone body applications with acceptable appearance and porosity.

The results of obtained flexural strength showed that the strength of all three samples was in this range due to the flexural strength of the ideal scaffolds for porous bone in the range of 2-12MPa. On the other hand, this strength reduction can be attributed to the amount of starch although the porosities were close to each other. As was expected, the interconnectivity of porosities increases with increasing of starch, which cause a reduction in strength.

3.5. Microstructure Study of Glass-Ceramic Scaffold

The scanning electron microscopy images of the glass-ceramic scaffolds are shown in Figure 7.

According to the ideal scaffolds, the average pore size for bone is higher than 100μm. The results showed that the average pore size of all three samples is almost within this range, but only the sample GCF5-665-P70 has interconnection of porosities, which is due to the high amount of porosity. Therefore, the GCF-665-P70 was selected as the appropriate porous scaffold body.

3.6. The Ability of Apatite Forming and Biodegradation

Variations of ion concentration with immersion time were investigated for various ionic species (Ca^{2+}, P^{5+}, Si^{4+}) and the results are presented in Figure 8.

The important points of this test are as below:

i) Higher concentrations of Ca were observed at longer immersion times in Figure 8a for the glass-ceramic leading to maximum leaching ability and surface reactivity of the respective glass-ceramic. The higher concentration of Ca in SBF at longer soaking times indicates that the modifier cations in the glass are no more exchanged with hydronium ions in the external solution (i.e. the inhibition of the biomineralization process) [34, 35].

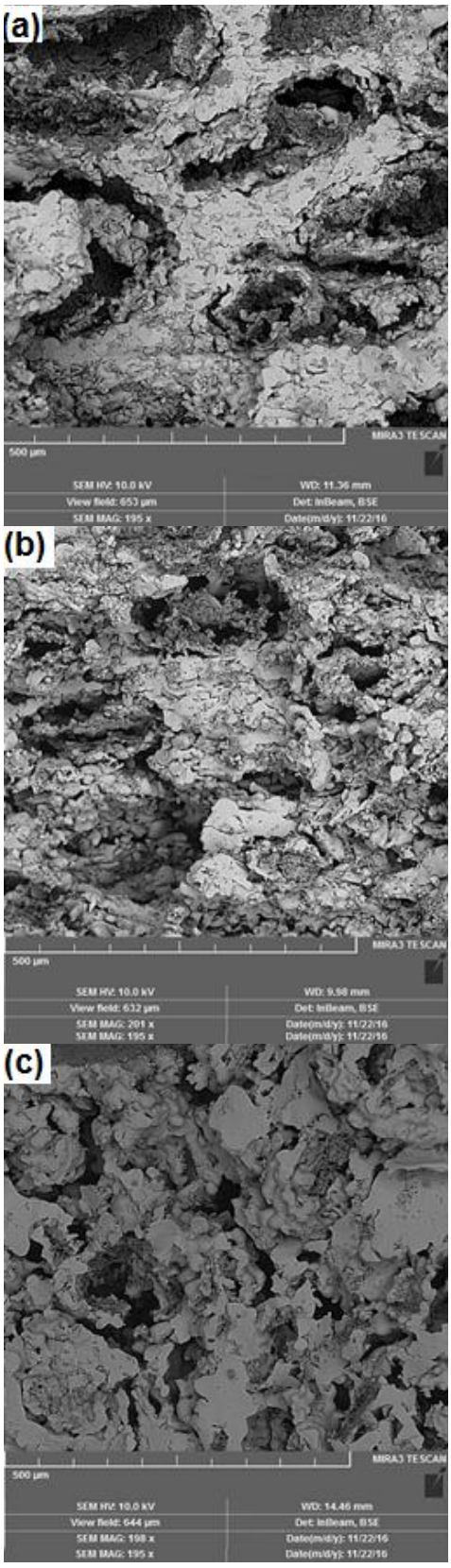

Figure 7. SEM images of glass-ceramic scaffolds a) GCF-640-P40 b) GCF-640-P50 c) GCF-665-P70, (All were heat-treated for 2 h)

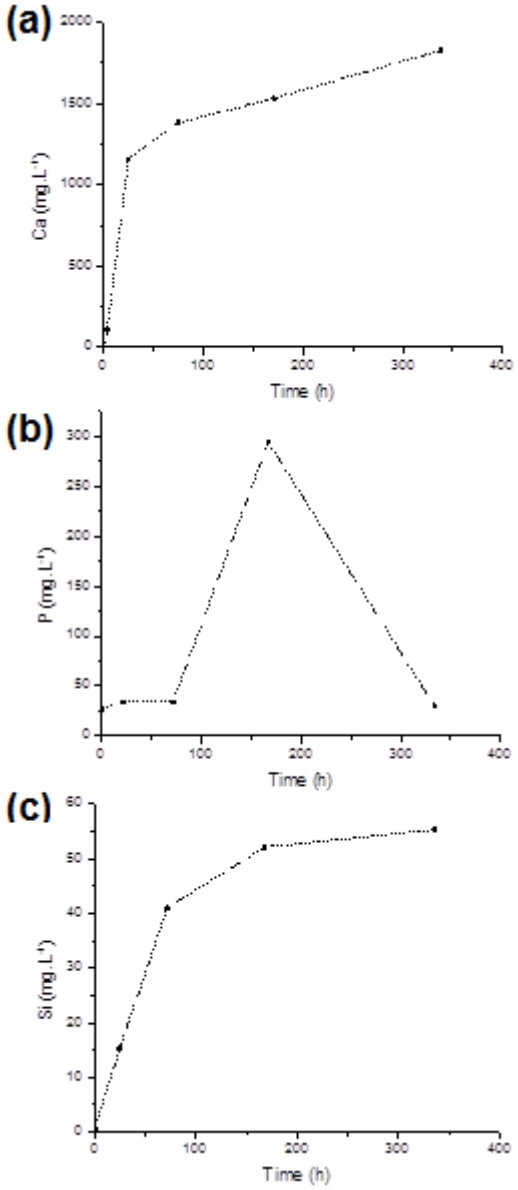

Figure 8. ICP plots of elemental concentration of (a) Ca, (b) P, and (c) Si, in SBF solution versus immersion time for the investigated GCs

ii) The sample exhibited higher concentration of phosphorus for the glass-ceramic Figure 8b once soaked in SBF, so that the highest phosphorus concentration was achieved after 7 days of soaking, beyond which time significantly lower concentrations were observed. The initial increase in the concentration of phosphorus might be related to two reasons including (1) the release of excessive soluble phosphate species, or (2) the rapid hydrolysis of low amounts of labile P–O–Si bridges from the remaining glassy phase in the fluid. These might have brought about two implications including (1) the local super-saturation of the solution, thereby facilitating the process via which, the HA content of the solution is precipitated, and/or (2) providing a buffer and hence, reducing surface acidity, which in turn would inhibit the bone-bonding [36, 37].

Moreover, it seems that the increase in the concentration of phosphorus occurs simultaneously with the initial stage of the reactivity mechanism features during which, the Si-OH groups was developed on the glass surface. At the other end of the spectrum, the lower concentration of phosphate following the maximum (Figure 8c) has been found to be linked to the movement of phosphorus ions to the glass surface where a layer of high calcium phosphate content was developed [34, 35].

iii) The higher concentration of Si ion was observed in the SBF solution with increasing the soaking time. Indeed, the surface Si-OH groups developed during the hydrolysis of the Si-O-Si contribute to the higher bioactivity of the resultant compound upon the decrease in silica content of glass-ceramic indirectly, which results in attenuating the hydroxyapatite-glass-ceramic interface energy [38].

Figure 9 demonstrates the SEM images of glass-ceramic samples after various soaking times in SBF solution. According to the images, an appetite-like layer was developed and well-grown on the surface of the samples following 14 days of soaking in SBF. According to the results of EDX analysis (Figure 10), phosphorus and calcium were the main constituents of these agglomerates. The weak Si peak could be attributed to the high content of SiO_2 in the layer developed on the bioactive surface [15, 39, 40].

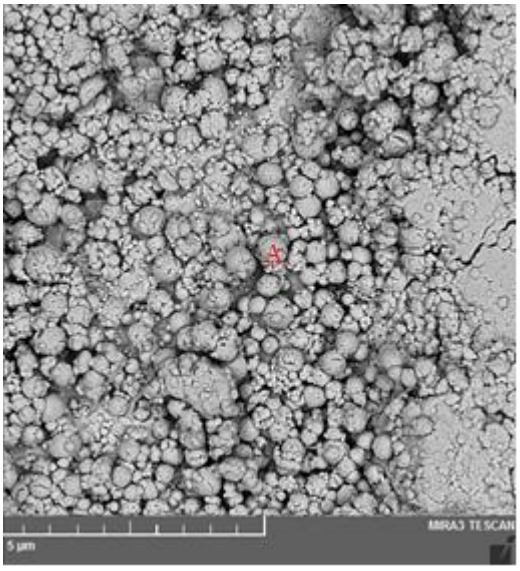

Figure 9. SEM image of glass-ceramic sample after immersion for 14 days in SBF solution (13000×)

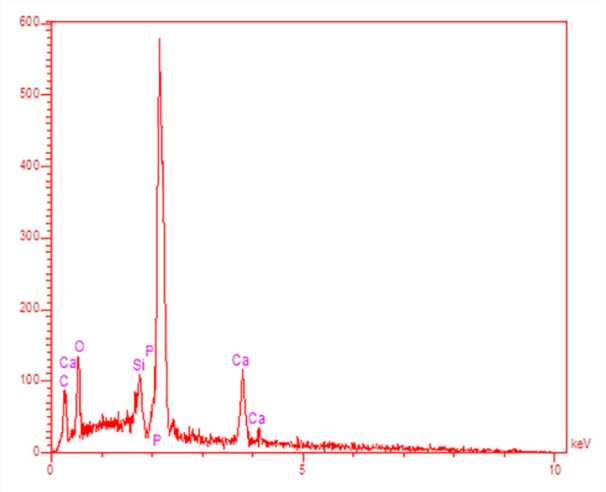

Figure 10. EDX analysis of glass-ceramic sample after 14 days of immersion in SBF solution (A area)

4. CONCLUSION

The purpose of this research was to prepare and characterize a macroporous glass-ceramic scaffold containing fluorapatite crystalline phase with composition near to 45S5. Macroporous bioactive glass-ceramic scaffolds were successfully obtained and the results of XRD, FTIR, and SEM analyses showed that the fluorapatite phase was formed and its amount increases with increasing the temperature.

The correct selection of the sintering temperature as well as the amount of porogen materials leads to a well-sintered specimen with good compromising between strength and highly porous structure. Furthermore, the prepared scaffold showed excellent bioactive behavior. In fact, in vitro studies showed that the CEL2 coating had high bioactivity due to the formation of a hydroxyapatite layer on its surface.

REFERENCES

1. Bravarone, C. V., Verné, E., Appendino , P., "Macroporous bioactive glass-ceramic scaffolds for tissue engineering", ***Journal of Materials Science: Materials in Medicine***, Vol. 17, No. 11, (2006), 1069-1078. https://doi.org/10.1007/s10856-006-0533-8
2. Mortera, R., Onida, B., Fiorilli, S., Cauda, V., Bravarone, C. V., Baino, F., Verné, E., Garrone, E., "Synthesis and Characterization of MCM-41 spheres inside bioactive glass-ceramic scaffold", ***Chemical Engineering Journal,*** Vol. 137, No. 1, (2008), 54-61. https://doi.org/10.1016/j.cej.2007.07.094
3. Renghini, C., Komlev, V., Fiori, F., Verné, E., Baino, F., Vitale-Brovarone, C., "Micro-CT studies on 3-D bioactive glass–ceramic scaffolds for bone regeneration", ***Acta Biomaterialia***, Vol. 5, No. 4, (2009), 1328-1337. https://doi.org/10.1016/j.actbio.2008.10.017
4. Vitale Bravarone, C., Baino, F., Verné, E., "Feasibility and tailoring of bioactive glass-ceramic scaffolds with gradient of porosity for bone grafting", ***Journal of Biomaterials Applications***, Vol. 24, No. 8, (2010), 693-712. https://doi.org/10.1177/0885328209104857
5. Jones, J. R., Hench, L. L., "Bioactive 3D scaffolds in regenerative medicine: the role of interface interactions" In ***Surfaces and Interfaces for Biomaterials***, Woodhead Publishing, (2005), 545-572. https://doi.org/10.1533/9781845690809.4.545
6. Jone, J. R., "Review of bioactive glass: From hench to hybrids", ***Acta Biomaterialia***, Vol. 9, No. 1, (2013), 4457-4486. https://doi.org/10.1016/j.actbio.2012.08.023
7. Vitale-Bravarone, C., Baino, F., Miola, M., Mortera, R., Onida, B., verné, E., "Glass-ceramic scaffolds containing silica mesophases for bone grafting and drug delivery", ***Journal of Materials Science: Materials in Medicine***, Vol. 20, No. 3, (2009), 809-820. https://doi.org/10.1007/s10856-008-3635-7
8. El-Meleigy, E., Van Noort, R., ***Glasses and Glass Ceramics for Medical Application***, Springer science & business media, New York, (2012). https://doi.org/10.1007/978-1-4614-1228-1
9. Anand, V., Singh, K. J., Kaur, K., "Evaluation of zinc and magnesium doped 45S5 mesoporous bioactive glass system for the growth of hydroxyl apatite layer", ***Journal of Non-Crystalline solids***, Vol. 406, (2014), 88-94. https://doi.org/10.1016/j.jnoncrysol.2014.09.050
10. Gerhardt, L. C., Boccaccini, A. R., "Bioactive glass and glass-ceramic scaffolds for bone tissue engineering", ***Materials***, Vol. 3, No. 7, (2010), 3867-3910. https://doi.org/10.3390/ma3073867
11. Kansal, I., Goal, A., Tulyaganov, D. U., Rajagopal, R. R., Ferreira, José M. F., "Structural and thermal characterization of $CaO–MgO–SiO_2–P_2O_5–CaF_2$ glasses", ***Journal of the European Ceramic Society***, Vol. 32, No. 11, (2012), 2739-2746. https://doi.org/10.1016/j.jeurceramsoc.2011.10.041
12. Wu, C., Chang, J., "Mesoporous bioactive glasses: structure characteristics, drug/growth factor delivery and bone regeneration application", ***Interface Focus***, Vol. 2, No. 3, (2012), 292-306. https://doi.org/10.1098/rsfs.2011.0121
13. Bellucci, D., Cannillo, V., Sola, A., Chiellini, F., Gazzarri, M., Migone, C., "Macroporous bioglass®-derived scaffolds for bone tissue regeneration", ***Ceramics International***, Vol. 37, No. 5, (2011), 1575-1585. https://doi.org/10.1016/j.ceramint.2011.01.023
14. Bellucci, D., Sola, A., Cannillo, V., "Bioactive glass-based composites for the production of dense sintered bodies and porous scaffolds", ***Materials Science and Engineering: C***, Vol. 33, No. 4, (2013), 2138-2151. https://doi.org/10.1016/j.msec.2013.01.029
15. Fiorilli, S., Baino, F., Cauda, V., Crepaldi, M., Vitale-Bravarone, C., Demarchi, D., Onida, B., "Electrophoretic deposition of mesoporous bioactive glass on glass-ceramic foam scaffolds for bone tissue engineering", ***Journal of Materials Science: Materials in Medicine***, Vol. 26, No. 1, (2015), 21. https://doi.org/10.1007/s10856-014-5346-6
16. Adams, L. A., Essien, E. R., Adesalu, A. T., Julius, M. L., "Bioactive glass 45S5 from diatom biosilica", ***Journal of Science: Advanced Materials and Devices***, Vol. 2, No. 4, (2017), 476-482. https://doi.org/10.1016/j.jsamd.2017.09.002
17. Hench, L. L., Wilson, J., ***An Introduction to Bioceramics, advanced series in ceramics***, Vol. 1, Singapore: World Scientific, (1993). https://doi.org/10.1142/2028
18. Peitl, O., Zanotto, E. D., Serbena, F. C., Hench, L. L., "Compositional and microstructural design of highly

bioactive P_2O_5-Na_2O-CaO-SiO_2 glass-ceramics", ***Acta Biomaterialia***, Vol. 8, No. 1, (2012), 321-332. https://doi.org/10.1016/j.actbio.2011.10.014

19. Clupper, D. C., Hench, L. L., Mecholsky, J. J., "Strength and toughness of tape cast bioactive glass 45S5 following heat treatment", ***Journal of the European Ceramic Society***, Vol. 24, No. 10-11, (2004), 2929-2934. https://doi.org/10.1016/s0955-2219(03)00363-7
20. Du, R., Chang, J., "Preparation and characterization of bioactive sol-gel-derived $Na_2Ca_2Si_3O_9$", ***Journal of Materials Science: Materials In Medicine***, Vol. 15, No. 12, (2004), 1285-1289. https://doi.org/10.1007/s10856-004-5736-2
21. Lefebvre, L., Chevalier, J., Gremillard, L., Zenati, R., Thollet, G., Bernache-Assollant, D., Govin, A., "Structural transformations of bioactive glass 45S5 with thermal treatments", ***Acta Materialia***, Vol. 55, No. 10, (2007), 3305-3313. https://doi.org/10.1016/j.actamat.2007.01.029
22. Ji, L., Si, Y., Li, A., Wang, W., Qiu, D., Zhu, A., "Progress of three-demensional macroporous bioactive glass for bone regeneration", ***Frontiers of Chemical Science and, Engineering***, Vol. 6, No. 4, (2012), 470-483. https://doi.org/10.1007/s11705-012-1217-1
23. Kokubo, T., Takadama, H., "How useful is SBF in predicting in vivo bone bioactivity?", ***Biomaterials***, Vol. 27, No. 15, (2006), 2907-2915. https://doi.org/10.1016/j.biomaterials.2006.01.017
24. Allahgoliyane, E., Rezvani, M., "Investigating the affect Factors in Manufacturing process of Porous Ceramic Glass Containing Crystalline Fluorapatite", In ***12th ICERS Congress Proceedings***, Iran, 30th April & 1st May 2019, Iranian Ceramic Society, (2019).
25. Farahinia, L., Rezvani, M., Alahgoliyan, E., "Optical characterization of oxyfluoride glasses containing different amounts of K_2O additive", ***Materials Research Bulletin***, Vol. 70, (2015), 461-467. https://doi.org/10.1016/j.materresbull.2015.05.015
26. Tahvildari, K., Esmaeili Pour, M., Ghammamy, S., Nabipour, H., "CaF_2 Nanoparticles: Synthesis and characterization", ***International Journal of Nano Dimension***, Vol. 2, No. 4, (2012), 269-273. https://doi.org/10.7508/ijnd.2011.04.008
27. Peitl, O., Zanotto, E. D., Hench, L. L., "Highly bioactive P_2O_5-Na_2O-CaO-SiO_2 glass-ceramics", ***Journal of Non-Crystalline Solids***, Vol. 292, No. 1-3, (2001), 115-126. https://doi.org/10.1016/s0022-3093(01)00822-5
28. Ghomi, H., Fathi, M. H., Edris, H., "Fabrication and characterization of bioactive glass/hydroxyapatite nanocomposite foam by gelcasting method", ***Ceramics International***, Vol. 37, No. 6, (2011), 1819-1824. https://doi.org/10.1016/j.ceramint.2011.03.002
29. Majhi, M. R., Pyare, R., Singh, S. P., "Studies on preparation and characterizations of CaO-Na_2O-SiO_2-P_2O_5 bioglass-ceramics substituted with Li_2O, K_2O, ZnO, MgO, and B_2O_3", ***International Journal of Scientific & Engineering Research***, Vol. 2, No. 9, (2011), 1-9. https://www.ijser.org/paper/Studies_on_preparation_and_characterizations.html
30. Doweidar, H., El-Damrawi, G., Mansour, E., Fetouh, R. E., "Structural role of MgO and PbO in MgO-PbO-B_2O_3 glasses as revealed by FT-IR: a new approach", ***Non-Crystalline Solids***, Vol. 358, No. 5, (2012), 941-946. https://doi.org/10.1016/j.jnoncrysol.2012.01.004
31. Thompson, I. D., Hench, L. L., "Mechanical properties of bioactive glasses, glass-ceramics and composites", ***Proceedings of the Institution of Mechanical Engineers, Part H: Journal of Engineering in Medicine***, Vol. 212, No. 2, (1998), 127-136. https://doi.org/10.1243/0954411981533908
32. Crovace, M. C., Souza, M. T., Chinaglia, C. R., Peitl, O., Zanotto, E. D., "Biosilicate® - A multipurpose, highly bioactive glass-ceramic. In vitro, in vivo and clinical trials", ***Journal of Non-Crystalline Solids***, Vol. 432, (2016), 90-110. https://doi.org/10.1016/j.jnoncrysol.2015.03.022
33. Vyas, V. K., Kumar, A. S., Singh, S. P., Pyare, R., "Effect of nickel oxide substitution on bioactivity and mechanical properties of bioactive glass", ***Bulletin of Materials Science***, Vol. 39, No. 5, (2016), 1355-1361. https://doi.org/10.1007/s12034-016-1242-7
34. Jones, J. R., Sepulveda, P., Hench, L. L., "Dose-dependent behavior of bioactive glass dissolution", ***Journal of Biomedical Materials Research: An Official Journal of The Society for Biomaterials, The Japanese Society for Biomaterials, and The Australian Society for Biomaterials and the Korean Society for Biomaterials***, Vol. 58, No. 6, (2001), 720–726. https://doi.org/10.1002/jbm.10053
35. Oliveira, J. M., Correia, R. N., Fernandes, M. H., "Surface modifications of a glass and a glass-ceramic of the MgO–3CaO-P_2O_5–SiO_2 system in a simulated body fluid", ***Biomaterials***, Vol. 16, No. 11, (1995), 849–854. https://doi.org/10.1016/0142-9612(95)94146-c
36. Karlsson, K. H., Fröberg, K., Ringbom, T., "A structural approach to bone adhering of bioactive glasses", ***Journal Non-Crystal Solids***, Vol. 112, No. 1-3, (1989), 69–72. https://doi.org/10.1016/0022-3093(89)90495-x
37. Zhang, H., Ye, X. J., Li, J. S., "Preparation and biocompatibility evaluation of apatite/wollastonite-derived porous bioactive glass ceramic scaffolds", ***Biomedical Materials***, Vol. 4, No. 4, (2009), 045007. https://doi.org/10.1088/1748-6041/4/4/045007
38. Tilocca, A., Cormack, A. N., de Leeuw, N. H., "The formation of nanoscale structures in soluble phosphosilicate glasses for biomedical applications: MD simulations", ***Faraday Discussions***, Vol. 136, (2007), 45-55. https://doi.org/10.1039/b617540f
39. Baino, F., Verné, E., Vitale-Brovarone, C., "Feasibility, tailoring and properties of polyurethane/bioactive glass composite scaffolds for tissue engineering", ***Journal of Materials Science: Materials in Medicine***, Vol. 20, No. 11, (2009), 2189-2195. https://doi.org/10.1007/s10856-009-3787-0
40. Hashmi, M. U., Shah, A. S., Elkady, A. S., "Effect of sintering time on crystallization, densification and in-vitro characteristics of bioactive glass ceramics", ***International Journal of Engineering Science and Innovative Technology***, Vol. 3, No. 1, (2014), 368-377. https://citeseerx.ist.psu.edu/viewdoc/download?doi=10.1.1.1047.2168&rep=rep1&type=pdf